Bifurcations of lattice structures

1983 J. Phys. A: Math. Gen. 16 673

(http://iopscience.iop.org/0305-4470/16/4/007)

J. Phys. A: Math. Gen. **16** (1983) 673–696. Printed in Great Britain

Bifurcations of lattice structures

T Janssen† and J A Tjon‡

† Institute for Theoretical Physics, University of Nijmegen, Toernooiveld, 6525 ED Nijmegen, The Netherlands

‡ Institute for Theoretical Physics, University of Utrecht, Princetonplein 5, 3584 CC Utrecht, The Netherlands

Received 26 April 1982

Abstract. Equilibrium configurations of a model for a crystal in one spatial dimension with anharmonic and up to third-neighbour harmonic interactions are related to orbits in a two- or four-dimensional space under a nonlinear symplectic mapping. In this way a connection is given with dynamical systems with two or three degrees of freedom. Depending on the parameters the orbits are smooth or stochastic. Their characterisation in terms of their fixed points and their Ljapunov exponents is given. The mapping shows a large number of bifurcations, of which one can distinguish various types, and these are discussed in the present paper.

1. Introduction

The problem of stability of dynamical systems has a long history. Since Poincaré and Birkhoff one has studied the effect of nonlinear perturbations, the perturbed solutions and their bifurcations. In the last decade important progress has been made on topics such as the existence of invariant surfaces, the transition to chaotic behaviour, the occurrence of series of period-doubling bifurcations, etc (Helleman 1980). Here we want to deal with a problem of lattice structure that is closely related to dynamical systems, although the connection is not immediately obvious.

Recently we have discussed a model for incommensurate crystal phases (Janssen and Tjon 1981, 1982b, the latter to be referred to as I), i.e. crystal phases where the positions of the atoms depart in a periodic way from the positions of a regular lattice structure, whereas the periodicity of this modulation is incommensurate with the underlying lattice. The model is a linear chain of classical particles with harmonic short-range (up to third neighbours) interaction and anharmonic nearest-neighbour interaction. If the third-neighbour interaction is absent, the condition that a configuration of the crystal should form a stationary point for the potential energy can be formulated as an area-preserving mapping of the plane. This mapping shows a number of interesting bifurcation phenomena which we have studied previously (Janssen and Tjon 1982a). In the present paper we discuss the relation between the bifurcations and the physical properties of the lattice model and we extend the discussion to the case where third-neighbour interactions play a role, which turns out to be of essential importance for the occurrence of incommensurate phases. The latter extension leads to a nonlinear symplectic mapping in a four-dimensional space. Concerning bifurcations this four-dimensional mapping has properties not present for the two-dimensional one.

The potential energy in the model is given by the expression

$$V = \sum_n [\tfrac{1}{2}\alpha(u_n - u_{n-1})^2 - \tfrac{1}{2}(u_n - u_{n-2})^2 + \tfrac{1}{2}\delta(u_n - u_{n-3})^2 + \tfrac{1}{4}(u_n - u_{n-1})^4] \tag{1.1}$$

where u_n is the displacement of the nth particle from its position in an equidistant array. The choice of the coefficients of the second and fourth terms is not a restriction but arises from an appropriate choice of energy and length units.

The first condition for having a state of minimal energy is the stationarity condition: $\partial V/\partial u_n = 0$. This leads to the following coupled set of nonlinear equations:

$$\alpha(2u_n - u_{n-1} - u_{n+1}) - 2u_n + u_{n-2} + u_{n-2} + \delta(2u_n - u_{n-3} - u_{n+3}) + (u_n - u_{n-1})^3 + (u_n - u_{n+1}^3) = 0. \tag{1.2}$$

If we introduce the difference coordinates

$$x_n = u_n - u_{n-1} \tag{1.3}$$

then after some arrangement of terms equation (1.2) becomes

$$(\alpha - 2)x_n - x_{n-1} - x_{n+1} + x_n^3 + \delta(3x_n + 2x_{n-1} + 2x_{n+1} + x_{n-2} + x_{n+2}) = (\alpha - 2)x_{n+1} - x_n - x_{n+2} + x_{n+1}^3 + \delta(3x_{n+1} + 2x_n + 2x_{n+2} + x_{n-1} + x_{n+3}) \tag{1.4}$$

or

$$(\alpha - 2 + 3\delta)x_n - (1 - 2\delta)(x_{n+1} + x_{n-1}) + x_n^3 + \delta(x_{n+2} + x_{n-2}) = f \tag{1.5}$$

for some constant f, independent of n.

For $\delta \neq 0$ one can express x_{n+2} in terms of $x_{n-2}, \ldots, x_{n+1}$ via

$$x_{n+2} = (2 - \alpha - 3\delta)(x_n/\delta) - (x_n^3/\delta) - [2 - (1/\delta)](x_{n+1} + x_{n-1}) - x_{n-2} + c \tag{1.6}$$

with $c = f/\delta$. In the following we shall restrict ourselves mainly to the case where $c = 0$. Introducing a vector v_n in R^4 with components $(x_{n+1}, x_n, x_{n-1}, x_{n-2})$ equation (1.6) determines a nonlinear transformation of R^4:

$$v_n \to v_{n+1} = Sv_n. \tag{1.7}$$

The character of the transformation can be seen from its linearised form:

$$DS = \begin{pmatrix} A & B & A & -1 \\ 1 & 0 & 0 & 0 \\ 0 & 1 & 0 & 0 \\ 0 & 0 & 1 & 0 \end{pmatrix} \tag{1.8}$$

where $A = (1 - 2\delta)/\delta$ and $B = (2 - \alpha - 3\delta - 3x_n^2)/\delta$. Because the determinant of DS is $+1$ the transformation preserves volume. Moreover, it is a symplectic transformation because it leaves invariant a symplectic form with matrix

$$\begin{pmatrix} 0 & 0 & 1 & 0 \\ 0 & 0 & -A & 1 \\ -1 & A & 0 & 0 \\ 0 & -1 & 0 & 0 \end{pmatrix}. \tag{1.9}$$

Notice that the symplectic form is constant: it does not depend on the position.

When $\delta = 0$ the recurrence relation (1.5) can be written as a nonlinear transformation in the plane R^2, because

$$x_{n+1} = (\alpha - 2)x_n + x_n^3 - x_{n-1} - f. \tag{1.10}$$

If one introduces a vector v_n with components (x_n, x_{n-1}), equation (1.10) determines a nonlinear transformation of the form (1.7). Its derivative is given by

$$DS = \begin{pmatrix} \alpha - 2 + 3x^2 & -1 \\ 1 & 0 \end{pmatrix}. \tag{1.11}$$

Because $\det(DS) = +1$ the mapping preserves area and is symplectic (every unimodular 2×2 matrix is symplectic). The cubic mapping (1.10) has been discussed by Janssen and Tjon (1982a). It follows that the lattice dynamical problem is intimately related to a discrete symplectic transformation. This transformation depends on the two parameters α and δ and shows, as a function of these, an interesting behaviour, which has consequences for the crystal.

The organisation of this paper is as follows. In § 2 we discuss the character of the transformation and of its fixed points in terms of the linearised mapping. The dynamical stability of the solutions of the equilibrium equations is related in § 3 to the character of the fixed points. In § 4 several orbits of the transformation are discussed to show the various invariant manifolds which can be found in this mapping. As a measure of the stochasticity of the orbits the Ljapunov exponents are calculated from some of the solutions. In § 5 various types of bifurcations are described which occur when the parameters are varied. In view of the recent interest in bifurcations in nonlinear systems these deserve a treatment on their own. Some concluding remarks are made in the final section.

2. Fixed points of the transformation

The character of the transformation S in equation (1.7) can be seen from its fixed points (FP), i.e. those vectors v for which $Sv = v$, and its cycles, i.e. orbits under S for a FP of S^N. Hence a cycle consists of the N points $S^n v$ $(n = 1, \ldots, N)$ where $S^N v = v$. Notice that every point of a cycle is a FP for S^N. The cycles correspond to periodic configurations of the linear chain: the solutions of equation (1.5) satisfy $x_{n+N} = x_n$ and consequently $u_{n+N} = u_n + \text{constant}$, which describes a dilatation of the chain (determined by the constant) combined with a modulation of period N.

When v is a FP of S^N a neighbourhood of v is mapped onto a neighbourhood via the linear transformation

$$DS^N = \prod_{n=1}^{N} DS_n. \tag{2.1}$$

For the mapping in R^2 $(\delta = 0)$ one obtains the eigenvalues of

$$DS^N = \prod \begin{pmatrix} \alpha - 2 + 3x_n^2 & 1 \\ 1 & 0 \end{pmatrix} \tag{2.2}$$

from the equation

$$\lambda^2 - T\lambda + 1 = 0 \tag{2.3}$$

where T is the trace of DS^N. Because T is real the eigenvalues appear in pairs λ, λ^{-1} which are both real or both on the unit circle in the complex plane. The eigenvalues $\frac{1}{2}[T \pm (T^2-4)^{1/2}]$ are both real if $|T| \geq 2$. When $|T|>2$ the FP is called hyperbolic. When $|T|<2$ the eigenvalues are on the unit circle and the FP is called elliptic because locally the mapping is an elliptic rotation. When $|T|=2$, the FP is called parabolic. Notice that because of the cyclic property of the trace, all points of one cycle have the same eigenvalues.

For the mapping in R^4 the eigenvalues of DS^N satisfy the equation

$$\lambda^4 - T\lambda^3 + \sigma\lambda^2 - T\lambda + 1 = 0 \tag{2.4}$$

where T is the trace and σ the second invariant of DS^N. Equation (2.4) holds because the transformation is symplectic. Because both T and σ are real, it follows that if λ is an eigenvalue then λ^{-1} and λ^* are also eigenvalues. Hence the FP in R^4 are of the following four types:

(i) there are four complex eigenvalues with $|\lambda| \neq 1$: $\lambda, \lambda^*, \lambda^{-1}, \lambda^{*-1}$;
(ii) there are four complex eigenvalues with $|\lambda| = 1$: $\lambda_1, \lambda_1^*, \lambda_2, \lambda_2^*$;
(iii) there are two complex and two real eigenvalues: $\lambda_1, \lambda_1^*, \lambda_2, \lambda_2^{-1}$; $|\lambda_1| = 1$;
(iv) there are four real eigenvalues: $\lambda_1, \lambda_1^{-1}, \lambda_2, \lambda_2^{-1}$.

The character of the FP is determined by the invariants T and σ:

(1) it is of type (i) if $T^2 - 4\sigma + 8 < 0$;
(2) it is of type (ii), (iii) or (iv) if $T^2 - 4\sigma + 8 > 0$:
  (2a) of type (ii) if $L_+ < 4$ and $L_- < 4$,
  (2b) of type (iii) if $L_+ > 4$ and $L_- < 4$, or $L_+ < 4$ and $L_- > 4$,
  (2c) of type (iv) if $L_+ > 4$ and $L_- > 4$,

where $L_\pm = T \pm (T^2 - 4\sigma + 8)^{1/2}$. The motion of points in the neighbourhood of a FP is determined by the type of the FP. For a FP of type (i), there is one plane with an inward spiralling, and another one with an outward spiralling. For a FP of type (ii) the motion consists of two independent elliptic rotations around the FP. For FP of types (iii) and (iv) there is a contracting and a dilating manifold, which is of dimension one for type (iii) and of dimension two for type (iv). Examples of these motions will be discussed in § 4.

3. Dynamical stability and character of the fixed points

Solutions of equation (1.2) correspond to stationary points of the potential energy. In order to have a minimum, however, one has to require that the linearised equations of motion around a stationary point have only real frequencies. We shall call this dynamical stability, in contrast to the stability of a FP of the symplectic mapping. A FP is mapping stable if a point near the FP stays so under an infinite number of iterations of the symplectic mapping. This happens, in general, when all eigenvalues are of absolute value unity, barring exceptional cases when the eigenvalues are $e^{\pi i}$, $e^{2\pi/3}$, or $e^{\pi i/2}$. So a FP is, in general, mapping stable, if it is of type (ii) (for the R^4 case) or elliptic (in the R^2 case).

The linearised equations of motion for small displacements ε_n from a stationary configuration $\{u_n\}$ are

$$\begin{aligned} m\ddot{\varepsilon}_n = {} & (2\alpha - 2 + 2\delta + p_n + p_{n+1})\varepsilon_n - (\alpha + p_{n+1})\varepsilon_{n+1} \\ & - (\alpha + p_n)\varepsilon_{n-1} + \varepsilon_{n-2} + \varepsilon_{n+2} - \delta\varepsilon_{n-3} + \delta\varepsilon_{n+3} \end{aligned} \tag{3.1}$$

where $p_n = 3x_n^2$. One can also view equation (1.5) as the equation for a stationary point of the potential

$$V = \sum [\tfrac{1}{2}\alpha x_n^2 + \tfrac{1}{4}x_n^4 - \tfrac{1}{2}(x_n + x_{n-1})^2 + \tfrac{1}{2}\delta(x_n + x_{n-1} + x_{n-2})^2 - fx_n]. \tag{3.2}$$

For small displacements ξ_n from a stationary configuration $\{x_n\}$ in this potential the linearised equations of motion are

$$\ddot{\xi}_n = (\alpha - 2 + 3\delta + 3x_n^2)\xi_n - (1 - 2\delta)(\xi_{n+1} + \xi_{n-1}) + \delta(\xi_{n+2} + \xi_{n-2}). \tag{3.3}$$

For periodic solutions $\{x_n\}$, corresponding to a cycle of the mapping S, the force constants in the linearised equations (3.3) have a period N and as a result the solutions are of the form

$$\xi_n \equiv \xi_{mN+p} = \xi_p \exp[\mathrm{i}(km - \omega t)] \tag{3.4}$$

where $0 \leq p < N$ and $0 \leq k < 2\pi$. Analogously the solutions of equation (3.1) are $\varepsilon_n = \varepsilon_p \exp[\mathrm{i}(km - \omega t)]$ in this case.

For a vanishing frequency ω equation (3.3) leads to the same mapping as equations (1.8) in R^4 and (1.11) in R^2. Hence, if for some value of k the corresponding $\omega(k) = 0$, one has the relation

$$\Delta v_{n+N} = \prod (DS)\Delta v_n = \exp(\mathrm{i}k)\Delta v_n \tag{3.5}$$

which implies that DS^N has an eigenvalue $\exp(\mathrm{i}k)$ and that the corresponding FP is of type (ii) or (iii) in R^4, or elliptic in R^2. Conversely, if DS^N has an eigenvalue on the unit circle $\lambda = \exp(\mathrm{i}k)$, then equation (3.3) has a zero-frequency solution with wavevector k. Hence a FP is of type (ii) or (iii), or elliptic, if and only if the dynamic equation (3.3) has a zero-frequency solution, i.e. if the corresponding configuration is unstable. Moreover, it is easily shown that equation (3.1) has a zero-frequency solution if and only if (3.3) has or if $k = 0$. The case of $k = 0$ corresponds to the translational mode which always exists for a crystal with potential energy (1.1), but not for one with potential energy (3.2).

The statement that elliptic FP in R^2 correspond to dynamically unstable configurations has been proved already by Aubry (1977). Its consequences, however, have not always been realised. The fact has immediate relevance for our lattice model. A configuration with a certain period may become unstable if the frequency of one of the eigenmodes goes to zero (a so-called soft mode) as a function of external parameters. It has been shown in I that the parameter α depends on the temperature. A soft mode develops if an eigenvalue of the mapping approaches the unit circle. The point on the unit circle $\exp(\mathrm{i}k)$, where the eigenvalue becomes of absolute value unity determines the wavevector k of the soft mode. For $\delta = 0$ there is only one pair of eigenvalues and the approach towards the unit circle can only happen via the real axis and then $k = 0$ or $k = \pi$. For $\delta \neq 0$ this is different for a transition from a FP of type (i) to a FP of type (ii). Hence a soft mode with incommensurate wavevector is only possible for $\delta \neq 0$. This explains why it is essential in our model to take third-neighbour interactions into account.

The FP corresponding to stable crystal configurations are certainly non-elliptic. Elliptic orbits under the mapping never correspond to stable situations. Moreover, it turns out that the most stable configurations are extremely unstable under the mapping: the points go off to infinity even for very small deviations from the FP.

4. Orbits

4.1. General characterisation

A Hamiltonian system with m degrees of freedom has a $2m$-dimensional phase space and a $(2m-1)$-dimensional energy surface. A surface of section then has $2m-2$ dimensions. The flow lines of the Hamiltonian vector field determine a discrete mapping of the surface of section onto itself which can be compared with our symplectic mapping. Here $m=2$ for $\delta=0$ and $m=3$ for $\delta\neq 0$. If the dynamical system is integrable then invariant tori exist which also persist for small perturbations. The invariant tori intersect the surface of section as an ellipse or a two-dimensional torus. In this way the discrete mapping traces an ellipse in the neighbourhood of an elliptic point in R^2 or a torus in the vicinity of a FP of type (ii) in R^4. The existence and dissolution of invariant tori for a dynamical system with $m=3$, with a nonlinear coupling between three anharmonic oscillators, have been discussed by Martinet and Magnenat (1981), Magnenat (1982) and Contopoulos *et al* (1982). Several of the orbits in our problem are rather similar to orbits in those references.

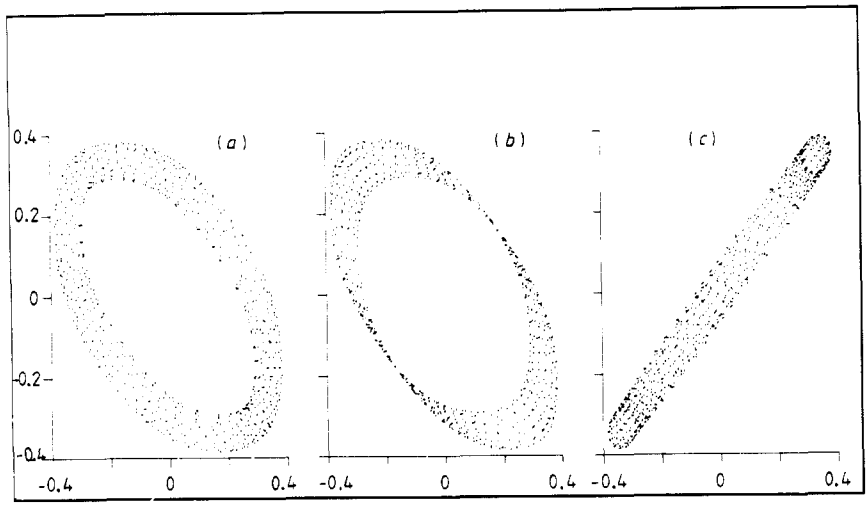

Figure 1. Orbit near a FP of type (ii) ($\alpha=0.9$, $\delta=1.0$) at the origin. Projections on different planes look quite different: (*a*) on x_n, x_{n+1}, (*b*) on x_n, x_{n+2}, (*c*) on x_n, x_{n+3}. Initial point: $x_1=0.25$, $x_2=0$, $x_3=-0.25$, $x_4=0.30$.

In figure 1 an example is given of the symplectic mapping (1.6) in the neighbourhood of a FP of type (ii). It is more difficult to present the orbits in four-dimensional than in two-dimensional space. We have chosen a projection on a plane x_n, x_{n-j} ($j=1, 2, 3$). The projections of a torus like that in figure 1 may be quite different. Apart from these orbits which fill an ellipse (or torus) there are divergent orbits for which $S^n v$ do not remain in a finite region of space. These orbits do not correspond to physical configurations of the crystal and therefore they are omitted. Finally there are orbits which are neither periodic (in which case the orbit is finite) nor restricted to a smooth curve. In R^2 this may happen in the neighbourhood of a hyperbolic point, where the orbit fills a region in space densely. This happens if the hyperbolic orbit is enclosed

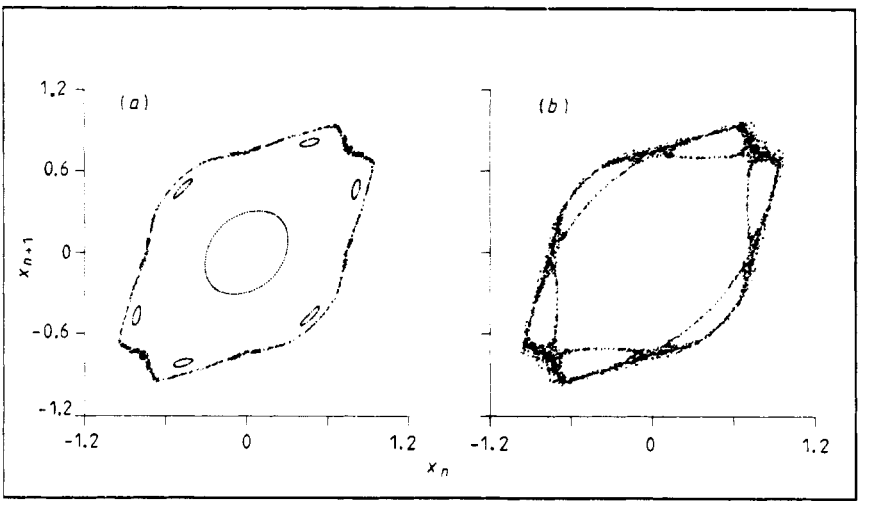

Figure 2. Orbits around an elliptic FP ($\alpha = 2.50$, $\delta = 0$). Near the FP the orbits are ellipses and smooth, further away they become more diffuse. The diffuse bands connect hyperbolic FP which are situated at the intersections of these bands. For the first few hundred iterations of the mapping only half of these bands are covered (a). Only after many iterations does the other half also appear (b). The six islands correspond to an $N = 6$ elliptic cycle.

inside an elliptic orbit. It also occurs if one moves away from an elliptic FP so that nonlinear effects become important and the invariant tori are washed out (figure 2). Enclosure by an invariant torus cannot happen in R^4 because a two-dimensional torus cannot enclose a region in four-dimensional space (Arnold diffusion). Nevertheless, it may also happen here that an orbit remains in the vicinity of a FP which is not of type (ii) (see figure 3).

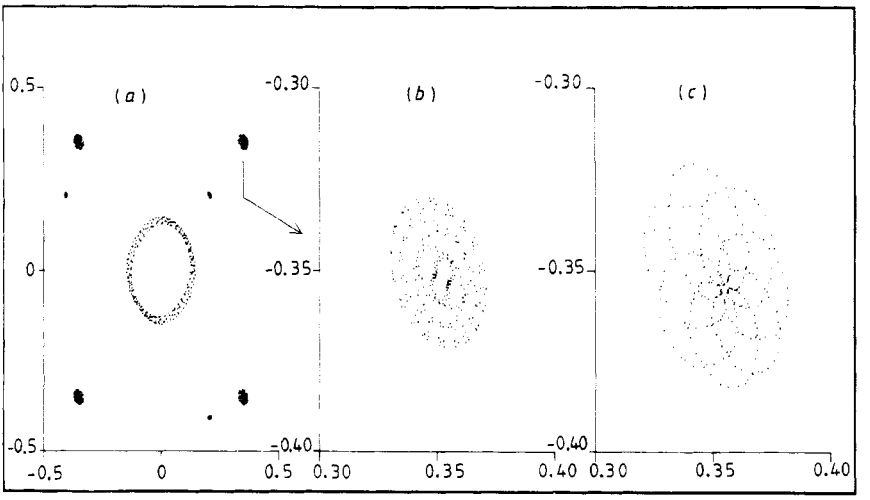

Figure 3. Orbits near FP of types (ii) and (i). (a) Orbit around an $N = 4$ and an $N = 3$ cycle, both of type (ii) ($\alpha = 0.876$, $\delta = 1$); (b) orbit around one of the $N = 4$ FP: the orbit is a torus ($\alpha = 0.876$, $\delta = 1$); (c) the FP has become of type (i), but nevertheless the orbit remains in the neighbourhood ($\alpha = 0.874$, $\delta = 1$).

The orbit in R^4 which fills a two-dimensional surface is not necessarily a simple torus. It may be something quite complicated as in figure 4. It is difficult to determine the topology of the latter orbit especially from the projections in figure 4. However, by taking sections one can verify that the orbit fills a two-dimensional surface. The structure is very distorted, as can be seen from the fact that the projections on two different planes are so different.

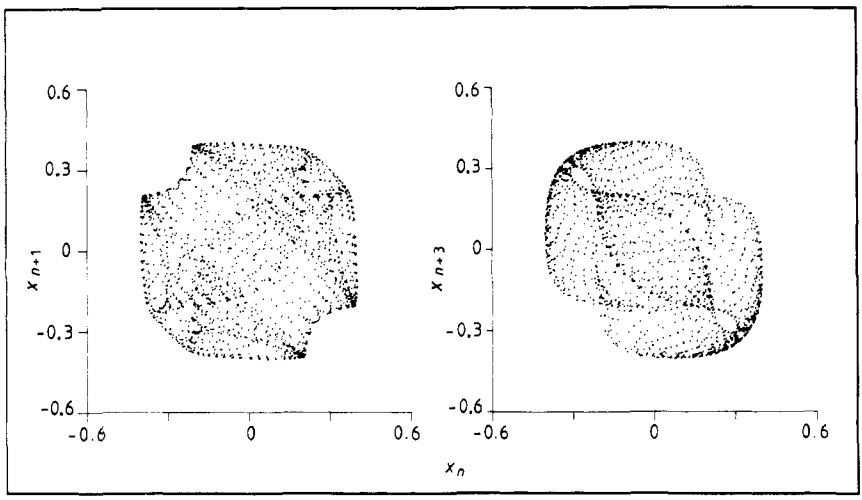

Figure 4. Two -dimensional orbit in R^4 ($\alpha = 0$, $\delta = 1$). Projection on two different planes. Initial point: $x_1 = x_2 = x_3 = x_4 = 0.1$.

If $\{x_n\}$ is an orbit, i.e. a solution of equation (1.5), another solution is found as $\{x'_n\}$ where

$$x'_n = x_{-n+p} \tag{4.1}$$

for some integer p. Moreover, if $f = 0$ in (1.5) another solution is $\{x'_n\}$ where

$$x'_n = -x_{n+p}. \tag{4.2}$$

The various values of p in (4.1) and (4.2) are simply renumberings of the points of the orbit, but, in general, there are four orbits with the same character if $f = 0$ (otherwise there are two). If an orbit is periodic the four cycles have the same eigenvalues. A special class of orbits is formed by those which are invariant under one of the operations (4.1) or (4.2). Hence one can distinguish four symmetric classes:

(I) $x_n = x_{-n+4}$: . . . e, d, c, b, a, b, c, d, e, . . . ,

(II) $x_n = x_{-n+3}$: . . . c, b, a, a, b, c, . . . ,

(III) $x_n = -x_{-n+3}$: . . . c, b, a, −a, −b, −c, . . . ,

(IV) $x_n = -x_{-n+4}$: . . . d, c, b, 0, −b, −c, −d, ...

Numerical calculations, reported in I, show that the configurations with the lowest energy always belong to one of these classes. There are, however, also examples of solutions of (1.5) which do not belong to one of these classes. Moreover, the classes may overlap. Restriction to these families reduces the determination of solutions to one- and two-parameter searches, for $\delta = 0$ and $\delta \neq 0$, respectively.

Among the solutions of (1.5) with a certain period N one may distinguish solutions with a different number of nodes ($2s$ with s a natural number). For the mapping the number s has the meaning of the number of times the orbit goes around the origin: it is the winding number. In I it was shown that solutions with period N and winding number s correspond to modulations with effective period N/s. Since an irrational number may be approximated arbitrarily closely by a fraction s/N, the incommensurate structures may be approximated by FP with large period N and large winding number s.

4.2. Special solutions

Equation (1.5) can only be solved analytically for periodic orbits with a small period. For larger periods one has to rely on numerical calculations. Since the general behaviour of the eigenvalues can already be seen in the small N cases, we shall discuss the solutions with $N=1$ and $N=2$ for $f=0$.

Solution A. An obvious FP for $N=1$ is $\{x_n=0\}$. This orbit belongs to each of the four symmetry classes (I)–(IV). For $\delta=0$ one has $T=\alpha-2$, for $\delta\neq 0$ $T=(1-2\delta)/\delta$ and $\sigma=(3\delta+\alpha-2)/\delta$. The character of this FP as a function of the parameters is indicated in figure 5(a). The corresponding crystal configuration is an equidistant array.

Solution B. Two other FP with $N=1$ are $\{x_n=(4-\alpha-9\delta)^{1/2}\}$ and $\{x_n=-(4-\alpha-9\delta)^{1/2}\}$. These orbits belong to the symmetry classes (I) and (II). For $\delta=0$ one has $T=10-2\alpha$ and for $\delta\neq 0$ $T=(1-2\delta)/\delta$ and $\sigma=-2(\alpha+12\delta-5)/\delta$. The character of the FP is illustrated in figure 5(b). The corresponding crystal configuration is again equidistant, however, with a different lattice constant, because $u_n=u_{n-1}+x_n=n(4-\alpha-9\delta)^{1/2}$.

Solution C. A solution of symmetry class (I) or (III) with period $N=2$ is $\{x_{2m}=-x_{2m-1}=(-\delta-\alpha)^{1/2}\}$. This cycle (with 2 FP of S^2) originates from the solution of type A along the line $\alpha=-\delta$, where the solution of type A has an eigenvalue $\lambda=-1$ (see figure 5(c)).

Solution D. Another cycle of length $N=2$ belonging to symmetry class (I) is $\{x_{2m}=c+d, x_{2m+1}=c-d\}$ or $\{x_{2m}=c-d, x_{2m+1}=c+d\}$, where $c^2=-\frac{1}{4}(2+\alpha-3\delta)$ and $d^2=\frac{1}{4}(6-\delta-13\delta)$. These two cycles (4 FP for S^2) originate from solution C for $\delta<\frac{1}{2}$ along $\alpha=-2+3\delta$, and from solution B for $\delta>\frac{1}{2}$ along $\alpha=6-13\delta$. The character is indicated in figure 5(d). Solution B has an eigenvalue $\lambda=-1$ along the line where solution D is created; solution C has an eigenvalue $\lambda=+1$ along the line where solution D originates from it.

In its turn solution D will give rise to cycles of period $N=4$ and this series of bifurcations continues. Since this behaviour is interesting in itself, we shall treat it in some detail in the next section.

For values of δ tending to zero, all solutions have at least two real eigenvalues. Actually, one of these eigenvalues goes to infinity and another to zero, whereas the two remaining eigenvalues tend to those for the R^2 mapping. This can be understood if one compares the eigenvalue equations for the R^2 and the R^4 mappings. The former is

$$\lambda^2-T\lambda+1=0 \qquad T=\alpha-2-3x^2 \tag{4.3}$$

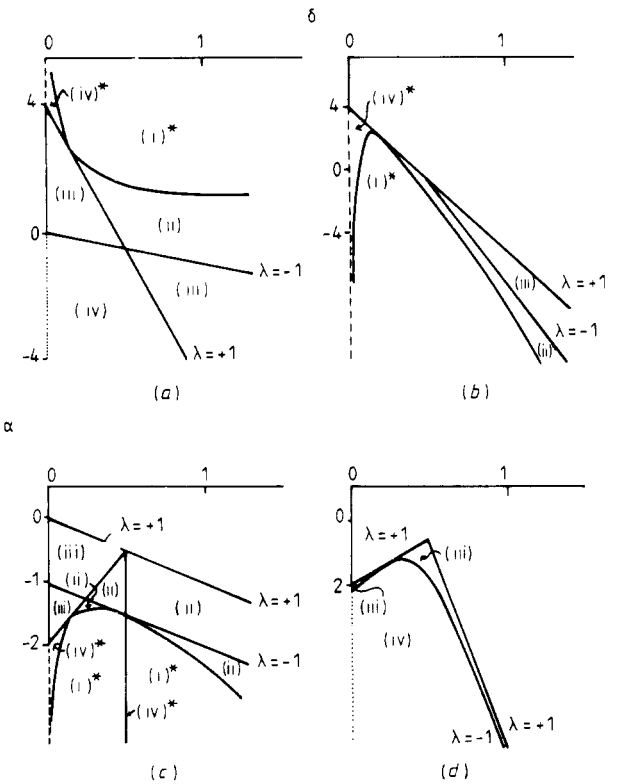

Figure 5. Type of the FP for some low-period solutions in the α, δ plane. (*a*) Solution A ($N=1$), (*b*) solution B ($N=1$), (*c*) solution C ($N=2$), (*d*) solution D ($N=2$). For $\delta=0$ the type is indicated by a full line (elliptic), a broken line (hyperbolic with λ positive) or a dotted line (hyperbolic with λ negative). Dynamical stability of a solution is indicated by an asterisk. (Solution D is always dynamically unstable.)

while the latter is

$$\lambda^4 - A(\lambda^3+\lambda) - B\lambda^2 + 1 \approx (\lambda^2 - T\lambda + 1)(\lambda^2 - a\lambda + 1) \tag{4.4}$$

where $a=[1-2\delta-(\alpha+3x^2)\delta]/\delta$, which tends to $1/\delta$ asymptotically. Hence the solutions of equation (4.4) are the two of equation (4.3) plus $\lambda_3 = 1/\delta$ and $\lambda_4 = \delta$. Hence if the FP in R^4 is of type (iii) the corresponding FP in R^2 is elliptic; if it is of type (iv) the corresponding one is hyperbolic.

Another special value is $\delta = 0.5$. As can be seen from equation (1.5) the chain splits into two uncoupled chains consisting of the particles at the odd and the even positions. The two sets of equations are

$$x_{n+2} = (1-2\alpha)x_n - 2x_n^3 - x_{n-2}. \tag{4.5}$$

One can rewrite equation (4.5) as a mapping in R^2 if one introduces $x_{2m} = 2^{-1/2}y_m$ or an analogous expression for the odd chain. Then

$$y_{m+1} = (1-2\alpha)y_m - y_m^3 - y_{m-1}. \tag{4.6}$$

The difference from equation (1.10) is a minus sign in front of the third-order term. If a solution of this equation has a period $N' = 2n$, one can write

$$x_{2m} = (-1)^m 2^{-1/2} y_m \tag{4.7}$$

and similarly for the odd chain. In that case one has for y_m

$$y_{m+1} = (2\alpha - 1)y_m + y_m^3 - y_{m-1} \tag{4.8}$$

which is the same as equation (1.10). Hence one obtains solutions to equation (4.5) from two even-period solutions of the R^2 mapping for a value $\alpha' = 2\delta + 1$. The solutions of the equations for one subchain (i.e. (4.7) or (4.8)) with small periods N_1 and N_2 are

A': $x_{2m} = 0$

B': $x_{2m} = a$ with $a^2 = -(\alpha + \frac{1}{2})$

C': $x_{2m} = (-1)^m a$ with $a^2 = -(\alpha - \frac{3}{2})$

D': $x_{4m} = a$, $x_{4m+2} = b$ with $a = c + d$, $b = c - d$ and $c^2 = \frac{1}{4}(1 - 2\alpha)$, $d^2 = \frac{1}{4}(5 - 2\alpha)$.

Corresponding solutions exist for the other chain. Since one can combine arbitrarily solutions of the subchains, the number of solutions for a given period is very large. For $N = 1$, one has the possibilities A'A' and B'B', for $N = 2$ there are A'B' and B'B' (one subchain with a plus sign, the other with a minus sign), and for $N = 4$ one can have A'C', A'D', B'C', B'D', C'C', C'D', D'D' (see also the appendix). These solutions also persist for $\delta \neq 0.5$, because the solutions depend on the parameters in a continuous way. As an example consider figure 6, where an orbit for $\delta = 0.5$ is compared with

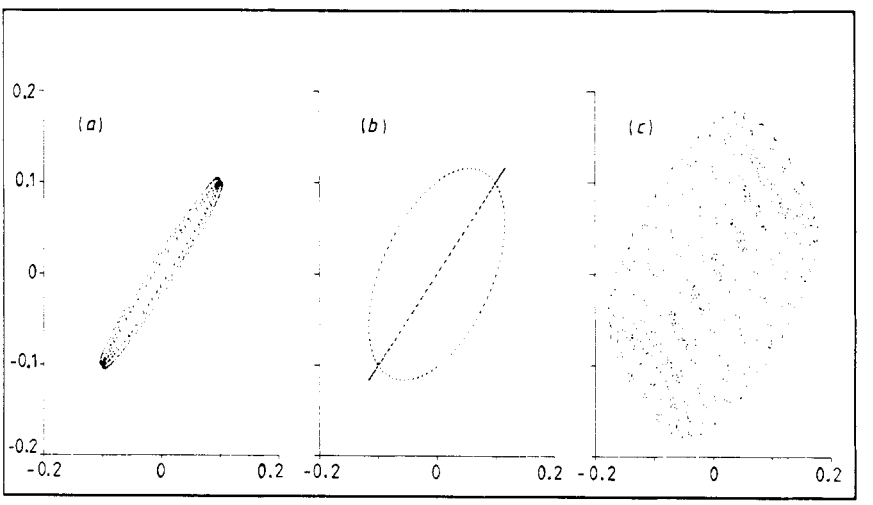

Figure 6. Orbits with the same initial point for different values of δ (projection is on the x_n, x_{n+1} plane). (*a*) $\alpha = 0$, $\delta = 0.45$; (*b*) $\alpha = 0$, $\delta = 0.50$; (*c*) $\alpha = 0$, $\delta = 0.55$.

orbits with exactly the same initial point for different values of δ. The eigenvalues of the origin are for $\delta = 0.5$ and $\alpha = 0$: $\exp(\frac{1}{3}i\pi)$, $\exp(\frac{5}{3}i\pi)$, $\exp(\frac{2}{3}i\pi)$ and $\exp(\frac{4}{3}i\pi)$. For $\delta \neq 0.5$ the formation of a torus is clearly visible. The fact that the figure for $\delta = 0.5$ consists of a straight line and an ellipse reflects the uncoupling of the two subchains. For $\delta \neq 0.5$ the orbits are deformed continuously.

4.3. Ljapunov characteristic numbers

It has been shown by Benettin *et al* (1976) that a measure of the stochasticity of orbits in a Hamiltonian flow is given by their Ljapunov characteristic numbers. For the discrete mapping S one can define these numbers for an orbit $\{S^n v; n = 1, 2, \ldots\}$ by

$$\rho = \lim_{n\to\infty} \rho_n \qquad \rho_n = n^{-1} \ln|(DS^n)x| \tag{4.9}$$

where x is a differential vector in v and $|\ |$ is the norm of the vector. For Hamiltonian flows on a compact manifold, where ρ is defined as $\lim\{\ln|DT^t x|/t\}$, it has been proved (Osseledec 1968) that this limit exists and takes one of a finite number of values. Moreover, for almost every vector in the tangent plane the limit is the maximum of those values. Benettin *et al* (1976) have given numerical evidence for the Henon–Heiles model that $\rho = 0$ for an orbit in an ordered region and that ρ tends to a constant in a chaotic region. Moreover, this constant depends only on the energy. Contopoulos *et al* (1978) find strong indications that the constant to which ρ tends also depends on the number of isolating integrals. This same result has also been found by Magnenat (1982) and Contopoulos *et al* (1982).

We have used the same characterisation for orbits under the discrete mapping. For an orbit of period N the Ljapunov characteristic number (LCN) is related to the largest eigenvalue (in absolute value) of the mapping DS^N. If a cycle is elliptic or of type (ii) the eigenvalues are on the unit circle and $\rho = 0$. For a hyperbolic cycle or a cycle of type (i), (iii) or (iv) ρ_n tends to $|\lambda|_{\max}^{1/N}$.

For a non-periodic orbit the LCN is a measure of the ordering. In general, ρ_n behaves asymptotically as

$$\rho_n \underset{n}{\to} An^{-L} \tag{4.10}$$

for some constant A and for a non-negative exponent L. We have calculated ρ_n for a number of typical orbits (figures 7 and 8). For an ordered orbit such as the ellipse

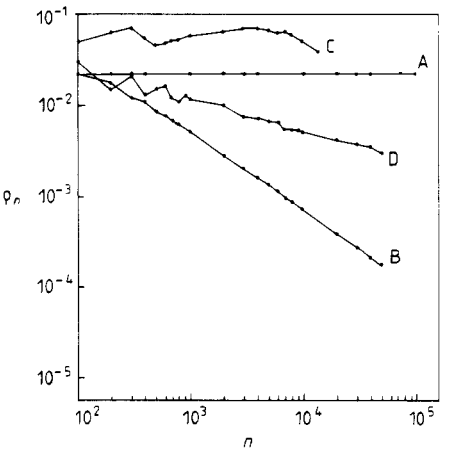

Figure 7. Ljapunov characteristic numbers for some typical orbits. A, hyperbolic FP, $\alpha = -0.05$, $\delta = 0$, $v = (0, 0)$; B, toroidal orbit of figure 4, $\alpha = 0.90$, $\delta = 1$, $v = (0.1, 0.1, 0.1, 0.1)$; C, chaotic orbit of figure 2, $\alpha = 2.5$, $\delta = 0$, $v = (0.74, 0.74)$; D, orbit of figure 14, $\alpha = 0.96$, $\delta = 1$, $v = (-0.201, 0.01, 0.201, 0)$.

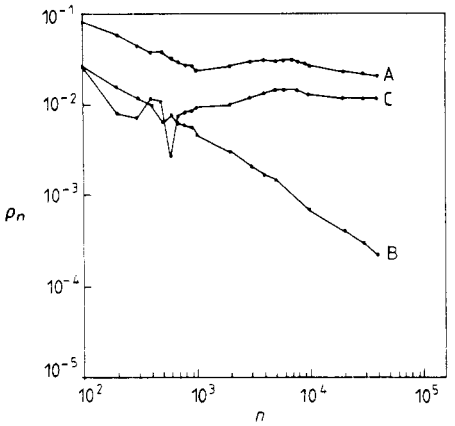

Figure 8. Ljapunov characteristic numbers for some orbits very close to each other at $\alpha = 0.99$, $\delta = 0$. A, near a hyperbolic point, $v = (1.005, 1.005)$; B, ordered orbit, $v = (0.92, 0.92)$; C, chaotic orbit, $v = (0.909, 0.909)$.

of figure 2(a) or the torus in figure 1, ρ_n tends to zero with $L = 1$. The behaviour of the LCN for the orbit of figure 4 favours the assumption that the orbit covers a two-dimensional surface. For a stochastic orbit such as the one in figure 2(b), the LCN tends to a constant. This also happens for an orbit which passes close to a hyperbolic FP under the condition that the orbit remains finite. An interesting type of orbit is the diffuse one in figure 11(b). For this orbit ρ_n tends to zero but $L \approx 0.35$. Presumably this orbit is not volume-filling but covers a lower-dimensional manifold. It turns out that a stochastic orbit often tends to infinity after many iterations. The point where the orbit breaks off is strongly influenced by rounding off errors and hence depends on the machine accuracy used.

Just as for the continuous mapping the convergence of ρ_n is not always monotonic. Especially in regions where ordered and disordered orbits are close to each other there are strong deviations from monotonic behaviour, even though ρ_n tends to zero with a mean exponent of $L = 1$. The picture becomes extremely complicated in these regions. As an example consider orbits near a hyperbolic $N = 4$ FP for $\alpha = 0.99$, $\delta = 0$ (figure 8). Ordered orbits starting from $v = (0.92, 0.92)$ or $(0.94, 0.94)$ are separated by chaotic orbits from $(1.005, 1.005)$ and $(0.91, 0.91)$. Moreover, very close to the latter there are again ordered orbits around cycles with $N = 40$ and $N = 48$ starting from $(0.903, 0.903)$ and $(0.917, 0.917)$, respectively. Hence the LCN can change very rapidly. There is also a pronounced difference in behaviour in ρ_n for the two orbits of figure 3.

The smoothness of an orbit can also be characterised by its dimension. To determine the (local) dimensionality one calculates the number $n(l)$ of points of the orbit inside a sphere of radius l as a function of this radius. One can then define the dimension d from $n(l) = \text{constant} \times l^d$. For a smooth curve in R^2, such as the ellipse in figure 2, one obtains $d = 1$ in this way, and $d = 2$ for a torus in R^4. This is also the case for the orbit in figure 4, which proves once more that this orbit covers a two-dimensional surface (figure 9). For stochastic orbits the slope of $\ln(n(l))$ against $\ln(l)$ is, in general, not a natural number. It should be noticed that for small values of l, the number of points inside the sphere is too small and the errors too large; for large values of l the global structure starts to be of importance. In the intermediate

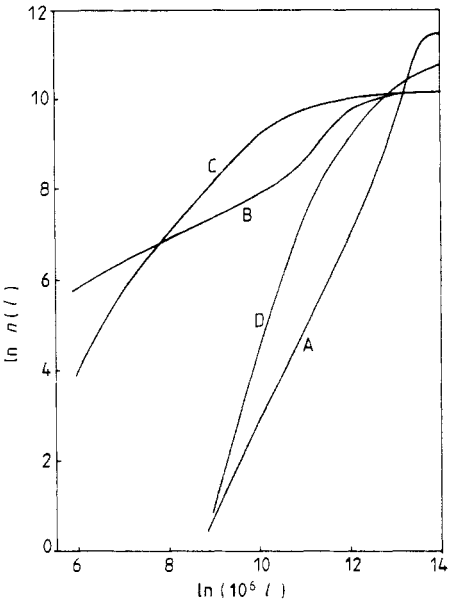

Figure 9. Number $n(l)$ of points of an orbit inside a sphere with radius l: the slope determines the dimension of the orbit. A, orbit of figure 4; B, orbit of figure 8(*b*); C, orbit of figure 8(*a*); D, orbit of $v = (-0.201, 0.01, 0.201, 0)$, $\alpha = 0.96$, $\delta = 1$ in figure 14(*b*).

region, however, the curve should be a straight line with a slope independent of the number of iterations in order to have a meaningful definition of d. Examples are given in figure 9. Curves B and C correspond to the orbits for which the Ljapunov exponents are given in figure 8. Their slopes are $d \approx 0.5$ and $d \approx 1.1$, respectively. The curvature of the right-hand side is caused by new global features entering the sphere (approximately 10 for $\ln(10^6 l)$). The curve correspondir g to the diffuse orbit in figure 14(*b*) has a slope significantly steeper than two, but due to the remaining curvature it is difficult to assign a dimension to this orbit.

5. Bifurcations

5.1. Types of bifurcations

For $\alpha > 1 + 1/4\delta$ the $N = 1$ FP $\{x_n = 0\}$ has four complex eigenvalues with $\lambda = 1$. So apart from the translation mode, the corresponding lattice configuration does not have a zero-frequency phonon. Explicit calculation shows that $\omega^2 > 0$, so that the basic configuration is stable. If the parameters α and δ are changed, the eigenvalues move in the complex plane. For α fixed and δ tending to zero two eigenvalues become zero and infinite while the other two are then given by the eigenvalues of the corresponding linearised mapping in R^2 for $\delta = 0$. The FP is hyperbolic with $\lambda > 0$ for $\alpha > 4$, elliptic for $0 < \alpha < 4$ and hyperbolic with $\lambda < 0$ for $\alpha < 0$. For $0 < \delta < \frac{1}{6}$ the four eigenvalues reach the real axis for $\alpha = 1 + 1/4\delta$. One pair moves towards $\lambda = +1$, which is reached for $\alpha = 4 - 9\delta$. Below this line there are two eigenvalues of modulus one and the basic configuration $(x_n = 0)$ is unstable. This means that for $0 < \delta < \frac{1}{6}$ a

soft mode develops with wavevector $k = 0$. For $\delta > \frac{1}{6}$ the eigenvalues move towards the unit circle which is reached at $\lambda = \exp(ik)$ with $\cos k = (1-2\delta)/4\delta$. Therefore in this case there is a soft mode with wavevector k.

At the point where the basic configuration becomes unstable, the FP $\{x_n = 0\}$ bifurcates: for $\delta < \frac{1}{6}$ two FP with $N = 1$ (solution B) branch off, both corresponding to a stable crystal configuration; for $\delta > \frac{1}{6}$ two cycles branch off. If $k = 2\pi s/N$, these cycles have period N. One cycle is of type (iii) and corresponds to an unstable configuration, the other is type (iv) and corresponds to a stable crystal configuration with period N. Since the winding number is s, the stable crystal structure is a modulated one with modulation wavevector $2\pi s/N$.

The branching off of new cycles at $\alpha = 1 + 1/4\delta$ is only the first in a long series of bifurcations. Because these bifurcations can give rise to new stable configurations, they are of importance for the dynamics of the crystal. Therefore we shall study them in some detail. Moreover, in view of the recent interest in bifurcations (Feigenbaum 1978, 1979, Eckmann 1981, Collet and Eckmann 1980), particularly in connection with turbulence problems, they deserve studying for their own sake.

Bifurcations for one-dimensional maps (Feigenbaum 1978, 1979, Collet and Eckmann 1980) and, to a lesser extent, for area-preserving and dissipative two-dimensional maps (Bountis 1981, Greene *et al* 1981, Collet and Eckmann 1981) have already received a lot of attention. In R^4 the subject of volume-preserving maps is even richer. Broadly speaking, one can distinguish two classes of bifurcations: those for which a cycle branches off from, in general, one of smaller period while the latter changes its character, and those for which the parent cycle does not change its character.

Type (*a*). Two eigenvalues come together at $\lambda = +1$ and a new cycle with the same period appears. An example is the $N = 1$ FP $\{x_n = 0\}$ for $\delta < \frac{1}{6}$. For $\alpha = 4 - 9\delta$ two eigenvalues collide at $\lambda = +1$ and two new FP (solution B) with $N' = 1$ start from this one. Another example is the $N = 2$ FP (solution C) for $\delta = 0$. It is elliptic for $-2 < \alpha < 0$. For α decreasing from 0 to -2 the eigenvalues move along the unit circle, pass through each other at $\lambda = -1$ and collide again for $\alpha = -2$. For this value two new elliptic FP with $N = 2$ branch off (solution D). The behaviour of the eigenvalues is illustrated in figure 10(*a*).

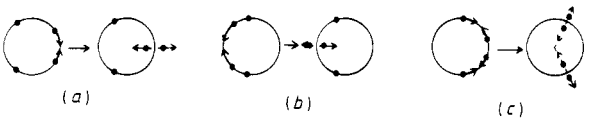

Figure 10. Change of the eigenvalues for bifurcations of types (*a*), (*b*) and (*c*).

Type (*b*). For this type two eigenvalues of a cycle of period N collide at $\lambda = -1$ and leave the unit circle along the real axis and a new cycle of period $N' = 2N$ is created. This type of period-doubling bifurcation has been studied extensively, for both one- and two-dimensional maps. An example is the $N = 1$ FP $\{x_n = 0\}$. If $\delta = 0$ the eigenvalues move along the unit circle for $0 < \alpha < 4$. For $\alpha = 0$ they collide at $\lambda = -1$. The FP becomes hyperbolic and a new $N = 2$ cycle (solution C) is created (figure 10(*b*)).

Type (*c*). In R^4 it may happen that the eigenvalues leave the unit circle for $\lambda \neq \pm 1$. The two pairs of eigenvalues collide and go off into the complex plane (figure 10(*c*)).

If this happens for $\lambda = \exp(2\pi i s/p)$ the original cycle of period N gives rise to two new cycles with period $N' = pN$. An example is the $N = 1$ FP $\{x_n = 0\}$ in the case where, for example, $\delta = 0.25$. For $\alpha > 2$ the eigenvalues are complex and not of modulus one. For $\alpha = 2$ they reach the unit circle at $\lambda = \exp(\frac{1}{3}\pi i)$ and move, for $\alpha < 2$, along the unit circle. Then DS^6 has four eigenvalues $+1$ for $\alpha = 2$. For $\alpha < 2$ there are two cycles of period $N = 6$, one of type (iii) (unstable configuration) and one of type (iv) (stable crystal configuration).

Type (*d*). For the preceding three cases the character of the parent cycle changes at the bifurcation. This is not so for a Birkhoff bifurcation, where a pair of eigenvalues moves along the unit circle and stays there. If the eigenvalues are $\exp(\pm 2\pi i s/p)$, new cycles of period $N' = pN$ may originate from the parent cycle of period N. If the N cycle is of type (ii) the two new cycles are types (ii) and (iii). If the N cycle is of type (iii), the new N' cycles are of types (iii) and (iv). In R^2 an elliptic N cycle leads to an elliptic and a hyperbolic N' cycle. An example is the $N = 1$ FP for $\delta = 0$. For $\alpha = 2$ its eigenvalues are $+i$ and $-i$. For $\alpha < 2$ an elliptic and a hyperbolic $N' = 4$ cycle appear, both of which move away from the origin. The eigenvalues of the hyperbolic N' cycle move along the real axis starting from $\lambda = +1$. The eigenvalues of the elliptic cycle move along the unit circle, also from $\lambda = +1$. In its turn the elliptic cycle may give rise to new cycles. For $\alpha = +1$ the eigenvalues leave the unit circle at $\lambda = +1$ and a bifurcation of type (*a*) takes place. The situation for $\alpha = 0.99$ is shown in figure 11. The origin is still an elliptic FP. The four islets outside the elliptic orbits correspond to the four FP of the $N' = 4$ cycle. They have just turned hyperbolic and in their neighbourhood there are the eight points of two elliptic $N' = 4$ cycles (figure 11(*b*)).

Type (*e*). A second type of bifurcation for which the character of the parent cycle does not change is what we have called 'inverse bifurcation'. Strictly speaking, it is not a real bifurcation. A cycle of period N has two eigenvalues on the unit circle.

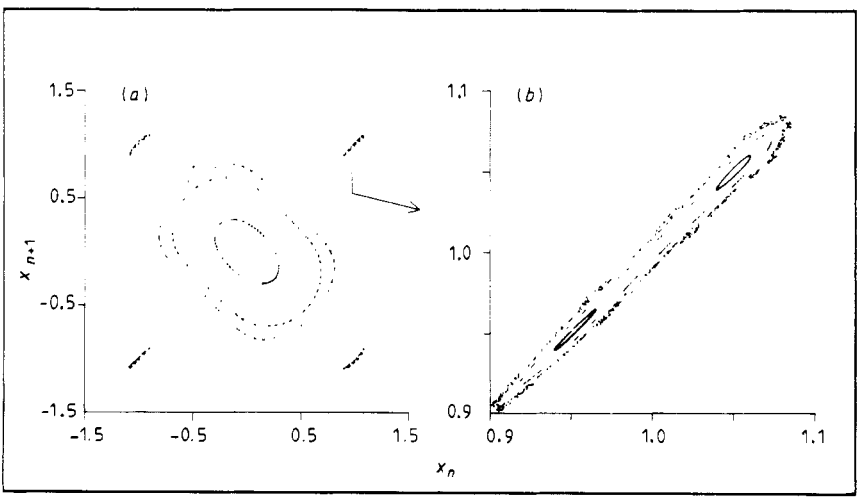

Figure 11. Bifurcations of types (*d*) and (*a*) (situation for $\alpha = 0.99$, $\delta = 0$). (*a*) FP at origin is elliptic, the four islets centred around the FP of an $N' = 4$ cycle, created at $\alpha = 2$, have become elongated. (*b*) One islet shows one $N' = 4$ FP in the centre that has become hyperbolic at $\alpha = 1$ and two elliptic $N' = 4$ FP created at $\alpha = 1$.

For $\alpha = \alpha_1$ these are $\exp(\pm 2\pi i s/p)$. For that value of α the N cycle absorbs and re-emits a cycle with period $N' = pN$ which was born for $\alpha = \alpha_2$. We have called this inverse bifurcation because the birth of the new cycles takes place beforehand. The rather complicated development can be illustrated by the example given in figures 12(*a*)–(*f*). The parent cycle has period $N = 3$. For $\alpha_1 = 0.09144\ldots$ its eigenvalues

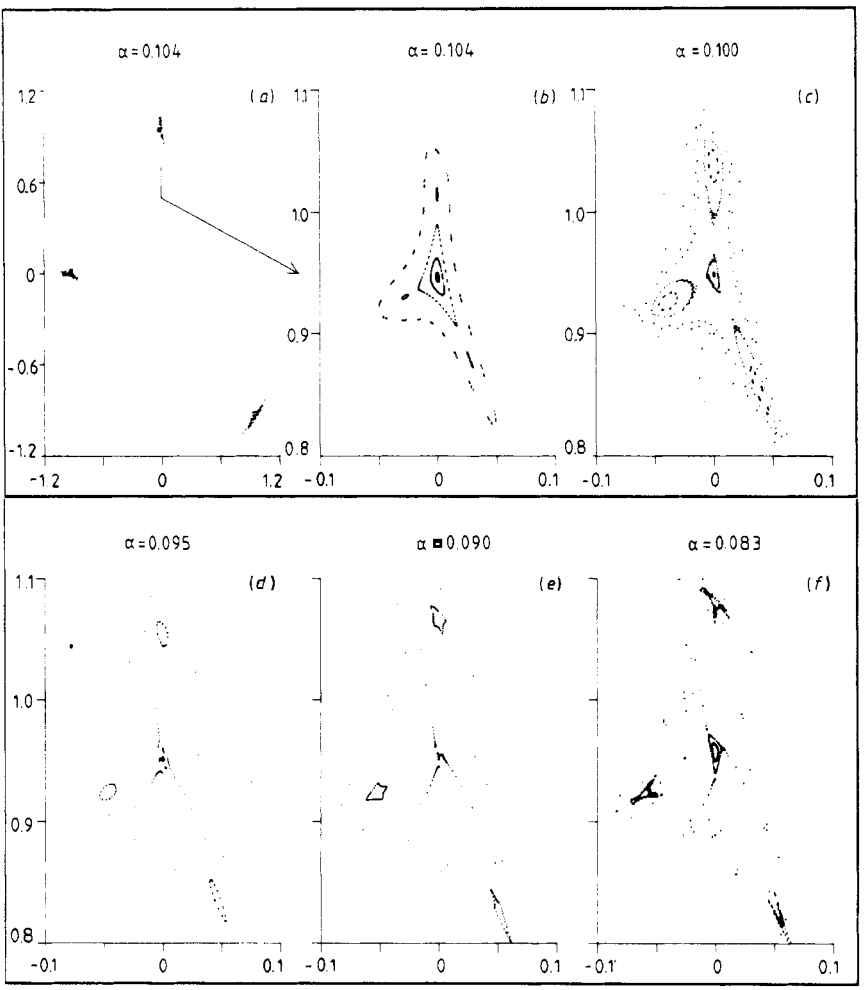

Figure 12. Inverse bifurcation. (*a*) Three islets around an elliptic $N = 3$ cycle; (*b*) in the vicinity of one $N = 3$ FP three hyperbolic and three elliptic FP with $N' = 9$ appear; (*c*) the hyperbolic FP approach the $N = 3$ FP, the elliptic ones move away; (*d*) the hyperbolic FP nearly collide; (*e*) the hyperbolic FP bounce back, the islets around the elliptic $N' = 9$ FP become deformed; (*f*) in the vicinity of each elliptic $N' = 9$ FP three hyperbolic and three elliptic FP with $N' = 27$ appear. ($\delta = 0$ in all cases, α is shown.)

are $\exp(\pm\frac{2}{3}\pi i)$. In its neighbourhood two new cycles with period $N' = 9$ are born for $\alpha_2 = 0.1043\ldots$: an elliptic one and a hyperbolic one (figure 12(*a*)). The hyperbolic cycle moves towards the $N = 3$ cycle in R^2 and reaches it for $\alpha = \alpha_1$. Its eigenvalues are $+1$ for α_1 and α_2. At $\alpha = \alpha_1$ the two cycles coincide. Then the hyperbolic one

bounces back and moves away from the parent cycle. The elliptic $N' = 9$ cycle also moves away from the $N = 3$ cycle. Its eigenvalues run along the unit circle, starting from $\lambda = +1$. For $\alpha = \alpha_1' = 0.08198\ldots$ they are again $\exp(\pm\frac{2}{3}\pi i)$. At that point it coincides with a hyperbolic $N'' = 27$ cycle created together with an elliptic one at $\alpha = \alpha_2' = 0.0833\ldots$. The formation of the $N'' = 27$ cycle is seen already in the form of the $N' = 9$ orbit (figure 12(e)): the ellipse develops three protrusions. In figure 12(f) the $N'' = 27$ cycles have already been formed. The story is then repeated.

5.2. Examples

Only bifurcations of type (c) are restricted to the four-dimensional mapping. The other four types do occur also in R^2 and for simplicity of presentation we have taken the examples from R^2 cases. To show that all types also occur for $\delta \neq 0$ we consider two other series of bifurcations.

As a first case we consider a series for $\delta = 1$ starting from the $N = 1$ FP of solution A. The behaviour of the eigenvalues is illustrated in figure 13(a). For $\alpha > 1.25$ the

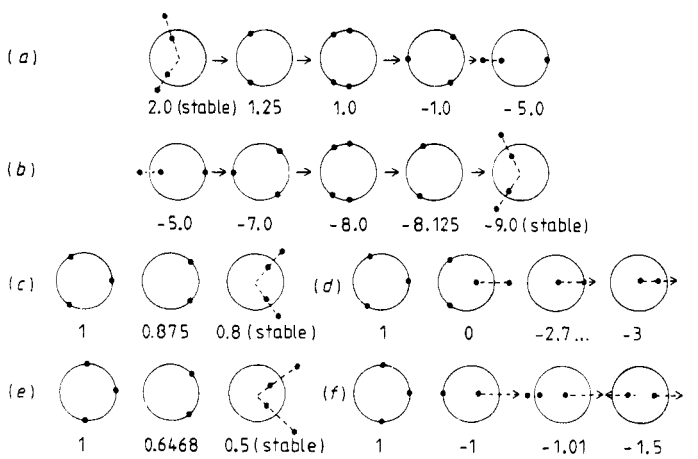

Figure 13. Change of the eigenvalue for some FP for varying α ($\delta = 1$). (a) The origin is an $N = 1$ FP; (b) solution B ($N = 1$); (c) the $N = 4$ FP of type (ii); (d) the $N = 4$ FP of type (iii); (e) the $N = 3$ FP of type (ii); (f) the $N = 3$ FP of type (iii). The $N = 3$ and $N = 4$ FP are created at $\alpha = 1$. (Arrows in (d) and (f) indicate large, real eigenvalues; 'stable' means dynamically stable.)

crystal is dynamically stable and the FP is of type (i). For $\alpha < 1.25$ the eigenvalues move along the unit circle, one pair clockwise, the other anticlockwise. For $\alpha = 1$ the eigenvalues are $\pm i$ and $\exp(\frac{2}{3}\pi i)$. At this point four new cycles start: two with period 4 and two with period 3 (figure 14). The bifurcation is of type (d). For $\alpha = -1$ two eigenvalues collide and leave the unit circle at $\lambda = -1$, whereas the other two are $\exp(\pm\frac{1}{3}\pi i)$. For this value of α a bifurcation of type (b) takes place (figure 14) that gives rise to an $N' = 2$ cycle (solution C), simultaneously with a bifurcation of type (d) that gives four $N' = 6$ cycles (one of type (i), one of type (ii) and two of type (iii): this is a situation where the minimal number of cycles does not appear). The two remaining eigenvalues of modulus one of the $N = 1$ FP collide at $\alpha = -5$ in $\lambda = +1$ and leave the unit circle. For $\alpha < -5$ the origin is a FP of type (iv) and two new $N' = 1$

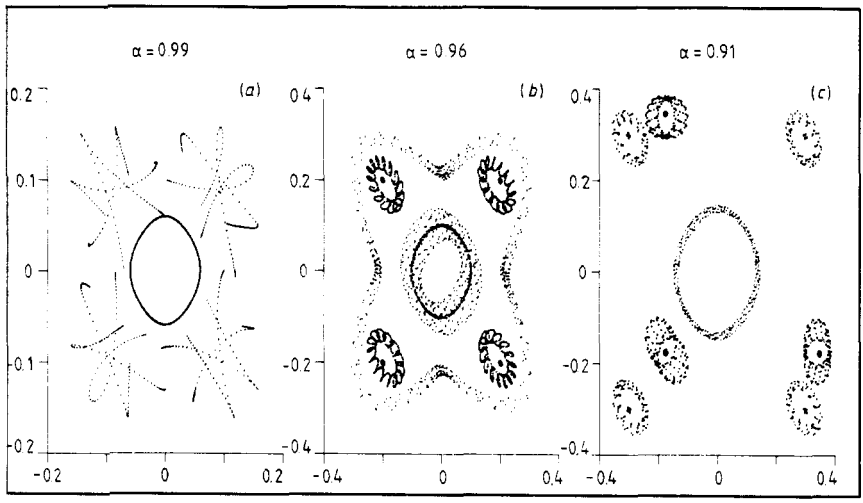

Figure 14. Creation of an $N' = 3$ cycle and an $N' = 4$ cycle at $\alpha = 1$, $\delta = 1$. (*a*) Sharp torus around the origin, three invariant curves around each $N' = 4$ FP; (*b*) the islets around the $N' = 4$ FP move away; the diffuse band connects the FP of type (iii); the tori are around those of type (ii); (*c*) the $N' = 3$ FP created at $\alpha = 1$ are also surrounded by a finite torus (nearly a cylinder), all FP move away. ($\delta = 0$ in all cases, α is shown.)

FP appear (solution B). This is an example of a bifurcation of type (*a*). The FP of solution B starts as type (iii) and its eigenvalues behave in exactly the same way as those of solution A, but in reverse order (figure 13(*b*)). The dynamically stable configurations of period 1 are solution A for $\alpha > 1.25$ and solution B for $\alpha < -8.125$.

The evolution of the $N = 3$ and $N = 4$ cycles born at $\alpha = 1$, $\delta = 1$ is illustrated in figures 13(*b*), (*c*), (*d*) and (*e*). The first $N = 4$ cycle is of type (ii) for $1 > \alpha > 0.875$. For $\alpha < 0.875$ it is of type (i) and the corresponding configuration is dynamically stable. The other $N = 4$ cycle is of type (iii) for $1 > \alpha > -2.7\ldots$. At $\alpha = -2.7\ldots$ it changes to type (iv) but the corresponding crystal configuration remains unstable because there is a whole phonon branch with imaginary frequencies. The same happens to the $N = 3$ cycles. One starts as type (ii) and changes to type (i) at $\alpha = 0.6468\ldots$, whereupon the crystal configuration becomes stable. The other remains unstable. Notice that for $\alpha = -1$ there is a bifurcation of type (*b*) from the $N = 3$ cycle to an $N' = 6$ cycle, whereas for the same value of α there is a bifurcation of type (*d*) from $N = 1$ to $N' = 6$. However, the two $N' = 6$ cycles are, of course, different (they have winding numbers 2 and 1, respectively). Another bifurcation near the same value of α (-1) is of type (*d*). It can be seen in figure 15, where the ring at $\alpha = -0.99$ has condensed to orbits around an $N' = 23$ cycle. This shows once more that constantly new cycles are born if α decreases.

An example of a bifurcation of type (*e*) for $\delta \neq 0$ is the bifurcation of solution C ($N = 2$) for $\delta = 0.25$. This cycle is created at $\alpha = -0.25$ for which value it has a double eigenvalue $\lambda = +1$ (it is of type (iii)). If α decreases two eigenvalues move along the unit circle, become degenerate ($\lambda = -1$ for $\alpha = -1.25$) and continue along the unit circle. For $\alpha = -1.25$ the cycle coincides with an $N' = 4$ cycle of type (iv) created at $\alpha = -1.0997\ldots$ together with an $N' = 4$ cycle of type (iii). The development of the two $N' = 4$ cycles is given in table 1. The cycle of type (iii) moves away and also in turn has a period-doubling bifurcation.

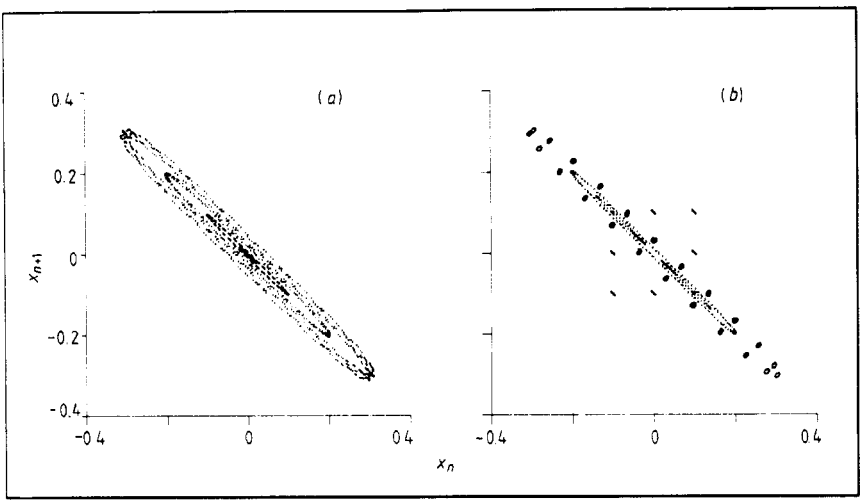

Figure 15. Simultaneous bifurcations of various types for $\alpha = -1$, $\delta = +1$. (*a*) The origin is an elliptic FP ($\alpha = -0.99$, $\delta = 1$); (*b*) the FP in the origin has become hyperbolic, an $N = 2$ elliptic cycle has branched off, as well as four $N = 6$ cycles of which one of type (iii) is shown; the annulus has condensed to tori around the FP of an $N = 23$ cycle ($\alpha = -1.01$, $\delta = 1$).

Table 1. Two $N = 4$ cycles created together for $\alpha = -1.0997\ldots$, $\delta = 0$. The configurations are $x_n = (a, -a, a, b)$.

First $N = 4$ cycle						Second $N = 4$ cycle					
α	a	b	λ_1	λ_3	Type	α	a	b	λ_1	λ_3	Type
−1.1	0.77	1.17	0.83 ± 0.56i	15.5	(iii)	−1.1	0.78	1.16	1.76	14.7	(iv)
−1.1034	0.74	1.19	−1	19.6	—	−1.107	0.81	1.14	7.66 ± 1.16i		(i)
−1.25	0.59	1.36	−39.8	51.8	(iv)	−1.175	0.93	1.11	4.39 ± 0.45i		(i)
						−1.2	0.96	1.03	2.39	4.34	(iv)
						−1.25	1	1	1 (4x)		—
						−1.30	1.04	0.98	−0.8 ± 0.6i	2.08	(iii)
						−1.303	1.05	0.97	−1	2.6	—
						−1.5	1.17	0.91	−21.2	12.2	(iv)

The creation of new FP is limited by a conservation law. Suppose v is an isolated FP of the transformation S. Then on the boundary $\partial\Omega$ of neighbourhood Ω of v a vector field is determined by $f(x) = Sx - x$. On $\partial\Omega$ this vector field does not have a zero. The topological index of this vector field (Sattinger 1973) does not depend on $\partial\Omega$, as long as no FP crosses the boundary. Since the FP depend smoothly on the parameters α and δ, this integer is a constant. Moreover, if there are n FP inside $\partial\Omega$ the index is just the sum of the indices for the n FP. The index of a FP can be calculated using

$$(f, v) = \mathrm{sgn}(\det(\partial f_i/\partial x_j)) \tag{5.1}$$

or, in terms of the quantities T and σ,

$$i(f, v) = \operatorname{sgn}(2 - 2T + \sigma). \tag{5.2}$$

For the mapping in R^2 the index is $+1$ for an elliptic FP or for a hyperbolic FP with negative eigenvalues; it is -1 for a hyperbolic FP with positive eigenvalues. In R^4 the index is $+1$ except when the FP is of type (iii) with positive real eigenvalues or of type (iv) with two positive and two negative eigenvalues. In these latter cases the index is -1. Because the index is a constant it does not change at a bifurcation: the sum of indices of the FP in a neighbourhood is the same before and after the bifurcation, as long as the new FP do not cross the boundary. This is the same reasoning as used in the discussion of the Hopf bifurcation (Sattinger 1973).

In R^2 for a bifurcation of type (a) this implies that an elliptic FP may only become hyperbolic (with positive eigenvalues) if, for example, two hyperbolic FP are annihilated or two elliptic FP are created. For a bifurcation of type (b) the index does not change, but as FP for S^2 the index changes from $+1$ to -1. This implies that two $N = 2$ elliptic FP (one two-cycle) have to be created. For bifurcations of types (d) and (e) of order p the index does not change either, not even for S^p. This means that p elliptic FP can only appear together with p hyperbolic ones (an elliptic and a hyperbolic p cycle), or that a hyperbolic FP of order p exists before and after the bifurcation (collision of FP).

In R^4 the conservation law allows the following possibilities.

Type (a): (ii) $\rightarrow$ (iii) + 2(ii); (ii) + 2(iii) $\rightarrow$ (iii); (iii) $\rightarrow$ (iv) + 2(iii); (iii) + 2(iv) $\rightarrow$ (iv) (under S).

Type (b): the same as type (a) under S^2.

Type (c): (i) $\rightarrow$ (ii) + p(iii) + p(iv) (under S^p).

Type (d): (ii) $\rightarrow$ (ii) + p(ii) + p(iii); (iii) $\rightarrow$ (iii) + p(iii) + p(iv) (under S^p).

Type (e): (ii) $\rightarrow$ (ii) + p(ii) + p(iii) followed by (ii) + p(iii) $\rightarrow$ (ii) + p(iii); (iii) $\rightarrow$ (iii) + p(iii) + p(iv) followed by (iii) + p(iv) $\rightarrow$ (iii) + p(iv) (under S^p).

These possibilities have been illustrated above by examples.

6. Concluding remarks

We have studied here discrete symplectic mappings in R^2 and R^4. Due to the fact that these mappings have their origin in a model for equilibrium configurations of a one-dimensional crystal, these mappings are not the simplest conceivable. In the first place they are cubic, in contrast to the quadratic mapping usually studied in R^2. This has implications for the motion of eigenvalues of the linearised mappings: in particular it gives rise to bifurcations where the period of solutions does not change. Furthermore, the four-dimensional mapping is singular in the parameter δ: for $\delta = 0$ the four-dimensional mapping is not defined, but then a two-dimensional mapping exists. Moreover, the two eigenvalues of the latter are the limit of two of the four eigenvalues in the four-dimensional mapping. Another limit is $\delta \rightarrow \infty$, because then the nonlinear terms become relatively less important.

The orbits under the symplectic mapping correspond to equilibrium crystal configurations, which are not necessarily dynamically stable. It turns out that there is a remarkable duality between the stability of a periodic orbit under the mapping and the dynamical stability of the crystal: if all the eigenvalues for the orbit are on the unit circle (a condition for mapping stability) the crystal configuration is unstable and, conversely, if the crystal is dynamically stable there are no eigenvalues for the

mapping on the unit circle. This has not always been realised: in the literature sometimes it is implicitly assumed that elliptic orbits correspond to stable physical configurations.

If the orbit traces a smooth curve (in R^2) or a smooth surface (in R^4), the Ljapunov exponent is zero. This implies that for such an orbit the differentials ξ_n form a solution of equation (3.3) with zero frequency. Since the Ljapunov exponent is zero the values for ξ_n are bounded and they correspond to a physically allowed displacement field. Hence for a smooth orbit, corresponding to a configuration without finite periodicity, there is a zero-frequency mode besides the acoustic one. Because of the vanishing of the Brillouin zone this does not necessarily mean that the configuration is unstable: the zero-frequency mode can be a phason mode.

If an eigenvalue of a linearised mapping approaches the unit circle, the corresponding crystal shows a soft mode. If there are interactions with first and second neighbours only, this soft mode appears in the centre or at the boundary of the Brillouin zone. As a consequence, in order to have a soft mode with incommensurate wavevector, interaction with third neighbours is essential.

In some of the bifurcations studied, two of the four real eigenvalues remain close to $+1$ for a fairly large α interval. A special case is the orbit of period $N = 3$ for $c \neq 0$ such that $\Sigma x_n = 0$. In this case there are, independent of α, two eigenvalues equal to $+1$. For the crystal this means that for $k = 0$ there is, besides the acoustic mode, another mode with frequency exactly equal to zero. It can be interpreted as a phason mode: the displacements can be described as shifts in the phase of the modulation function. If the energy of the equilibrium configuration does not depend on the phase, there is a point-wise invariant line under S^N.

It turns out that all stable crystal configurations correspond to orbits which are created at the origin. Sometimes these start as dynamically unstable and become stable only at a certain distance from the origin. The eigenvalues of the corresponding orbit always have an absolute value not equal to one and the orbits are very unstable: even a very small deviation leads to an unbounded (unphysical) orbit. For low enough values of the parameter α there is an infinite number of stable equilibrium configurations.

It should be stressed that there are several roads to stochasticity in the regions of R^2 and R^4: in the first place there are geometric series of bifurcations (Feigenbaum sequences) which lead to an infinite number of periodic orbits arbitrarily close to a parent orbit; in the second place there are simultaneously a large number of bifurcating families such that there are regions densely filled with periodic orbits of all kinds.

The multidimensional mapping has many bifurcation features in common with the two-dimensional one. In addition bifurcations are possible where pairs of eigenvalues collide and leave the unit circle. As a consequence, a series of bifurcations may not continue indefinitely but may break off for some period.

The picture arises of an ever-continuing network of bifurcations with increasing density. In fact the R^2 and R^4 get an infinite number of cycles in a finite region of space. Among the many bifurcations some behave in a regular way as geometric series. These will be the subject of a forthcoming paper.

The ever-increasing number of solutions has important consequences for the properties of the crystal. The large number of stable equilibrium configurations leads to a slowing down of the approach to equilibrium, especially so if a stable configuration is surrounded by the very large number of solutions created in a bifurcation series, because these solutions remain in the neighbourhood due to the geometric character.

Because the orbits bifurcated from one single orbit are, in general, only metastable or even unstable, we do not expect that those 'irregular' crystals, i.e. modulated crystals with a large number of modulation vectors, correspond to stable configurations. This is in contrast to a recent proposal by Ruelle (1982).

Appendix

For $\delta = 0.5$ the recurrence relation (1.6) reduces to (4.5). Hence the chain consists of two uncoupled subchains. If $x_{2m} = z_m$ the relation

$$z_{m+1} = (1-2\alpha)z_m - 2z_m^3 - z_{m-1} \tag{A1}$$

can be interpreted as an area-preserving mapping in R^2. Analogously one obtains such a mapping for the odd positions. If there is a cycle of period N' for (A1) and N' is even, then the cycle is in 1–1 correspondence to one of (1.10) via (4.6). One then gets equation (4.7) which is the same as (1.10) with $\alpha' - 2 = 2\alpha - 1$. Hence cycles for α' at $\delta = 0$ give cycles for the subchain at $\delta = 0.5$ and

$$\alpha = \alpha' - \tfrac{1}{2}. \tag{A2}$$

A FP for (1.6), i.e. $N = 1$, is only possible if both subchains are identical. Then one has again solutions A and B: $\{x_n = 0\}$ and $\{x_n = a\}$ with $a^2 = -\alpha - \frac{1}{2}$, respectively. For cycles with an even period N one may write

$$DS^N = \prod_{m=1}^{N/2} \begin{pmatrix} 1-2\alpha-6x_{2m}^2 & 0 & -1 & 0 \\ 0 & 1-2\alpha-6x_{2m+1}^2 & 0 & -1 \\ 1 & 0 & 0 & 0 \\ 0 & 1 & 0 & 0 \end{pmatrix}. \tag{A3}$$

Hence the eigenvalues are the solutions of

$$\lambda^4 - T(\lambda^3 + \lambda) + \sigma\lambda^2 + 1 = (1 - \chi_0\lambda + 1)(1 - \chi_1\lambda + 1) = 0 \tag{A4}$$

where the coefficients χ_0 and χ_1 are given by

$$\chi_j = \operatorname{Tr} \prod_{m=1}^{N/2} \begin{pmatrix} 1-2\alpha-6x_{2m+j}^2 & -1 \\ 1 & 0 \end{pmatrix}. \tag{A5}$$

If the period of the subchain is $N' = N/2$, then (A5) can be written as

$$\chi_j' = \operatorname{Tr} \prod_{m=1}^{N'} \begin{pmatrix} \alpha' - 2 + 3y_m^2 & -1 \\ 1 & 0 \end{pmatrix} \tag{A6}$$

where α' is given by (A2) and y_m^2 by (4.7). Then the four eigenvalues of DS^N are the two for $DS^{N'}$ in one subchain and two for the other one.

References

Aubry S 1977 *On the Dynamics of Structural Phase Transition Lattice Locking and Ergodic Theory* unpublished

Benettin G, Galgani L and Strelcyn J M 1976 *Phys. Rev.* A **14** 2338

Bountis T C 1981 *Physica* **3D** 577

Collet P and Eckmann J P 1980 *Iterated Maps on the Interval as Dynamical Systems* (Boston: Birkhaeuser)
—— 1981 *Physica* **3D** 457
Contopoulos G, Galgani L and Giorgilli A 1978 *Phys. Rev.* A **18** 1183
Contopoulos G, Magnenat P and Martinet L 1982 *Invariant Surfaces and Orbital Behaviour in Dynamical Systems of 3 Degrees of Freedom II* to be published
Eckmann J P 1981 *Rev. Mod. Phys.* **53** 643
Feigenbaum M J 1978 *J. Stat. Phys.* **19** 25
—— 1979 *J. Stat. Phys.* **21** 669
Greene J M, Mackay R S, Vivaldi F and Feigenbaum M J 1981 *Physica* **3D** 468
Helleman R H G 1980 *Fundamental Problems in Statistical Mechanics* vol 5, ed E G D Cohen (Amsterdam: North-Holland)
Janssen T and Tjon J A 1981 *Phys. Rev.* B **24** 2245
—— 1982a *Phys. Lett.* **87A** 139
—— 1982b *Phys. Rev.* B **25** 3767
Magnenat P 1982 *Numerical Study of Periodic Orbit Properties in a Dynamical System with Three Degrees of Freedom* to be published
Martinet L and Magnenat P 1981 *Astron. Astrophys.* **96** 68
Osseledec V I 1968 *Tr. Moscow. Math. Obsch.* **19** 179
Ruelle D 1982 *Do There Exist Turbulent Crystals*? preprint
Sattinger D H 1973 *Topics in Stability and Bifurcation Theory* Lecture Notes in Mathematics 309 (Berlin: Springer)